High-Throughput Phenotyping of Maize Leaf Physiological and Biochemical Traits Using Hyperspectral Reflectance[1][OPEN]

Craig R. Yendrek, Tiago Tomaz, Christopher M. Montes, Youyuan Cao, Alison M. Morse, Patrick J. Brown, Lauren M. McIntyre, Andrew D. B. Leakey, and Elizabeth A. Ainsworth*

Carl R. Woese Institute for Genomic Biology (C.R.Y., T.T., C.M.M., Y.C., P.J.B., A.D.B.L., E.A.A.), Department of Plant Biology (C.M.M., A.D.B.L., E.A.A.), and Department of Crop Sciences (P.J.B.), University of Illinois at Urbana Champaign, Urbana, Illinois 61801; Plant Protection Department, Fujian Agriculture and Forestry University, Fuzhou 350002, China (Y.C.); Department of Molecular Genetics and Microbiology and Genetics Institute, University of Florida, Gainesville, Florida 32610 (A.M.M., L.M.M.); and Global Change and Photosynthesis Research Unit, United States Department of Agriculture-Agricultural Research Service, Urbana, Illinois 61801 (E.A.A.)

ORCID ID: 0000-0002-3199-8999 (E.A.A.).

High-throughput, noninvasive field phenotyping has revealed genetic variation in crop morphological, developmental, and agronomic traits, but rapid measurements of the underlying physiological and biochemical traits are needed to fully understand genetic variation in plant-environment interactions. This study tested the application of leaf hyperspectral reflectance (λ = 500–2,400 nm) as a high-throughput phenotyping approach for rapid and accurate assessment of leaf photosynthetic and biochemical traits in maize (*Zea mays*). Leaf traits were measured with standard wet-laboratory and gas-exchange approaches alongside measurements of leaf reflectance. Partial least-squares regression was used to develop a measure of leaf chlorophyll content, nitrogen content, sucrose content, specific leaf area, maximum rate of phospho*enol*pyruvate carboxylation, [CO_2]-saturated rate of photosynthesis, and leaf oxygen radical absorbance capacity from leaf reflectance spectra. Partial least-squares regression models accurately predicted five out of seven traits and were more accurate than previously used simple spectral indices for leaf chlorophyll, nitrogen content, and specific leaf area. Correlations among leaf traits and statistical inferences about differences among genotypes and treatments were similar for measured and modeled data. The hyperspectral reflectance approach to phenotyping was dramatically faster than traditional measurements, enabling over 1,000 rows to be phenotyped during midday hours over just 2 to 4 d, and offers a nondestructive method to accurately assess physiological and biochemical trait responses to environmental stress.

Meeting future global food demand is projected to require a doubling of agricultural output by 2050 (Tilman et al., 2011). Climate change will exacerbate this challenge by intensifying the exposure of field crops to abiotic stress conditions, including rising temperature, increased drought, flooding, and air pollution (Christensen et al., 2007). In order to more rapidly adapt crops to the future growing environment, diverse germplasm must be meaningfully assessed in field conditions. However, our capacity to phenotype thousands of crop genotypes in a field environment is constrained by available high-throughput phenotyping platforms (Furbank and Tester, 2011; Araus and Cairns, 2014), and our ability to adapt crops to global climate change requires facilities that accommodate hundreds of genotypes in a realistic environment (Ainsworth et al., 2008).

This study provides proof of concept for one approach for high-throughput phenotyping of leaf physiological responses to global change using hyperspectral reflectance spectra of diverse maize (*Zea mays*) inbred and hybrid lines grown at ambient and elevated ozone concentrations ([O_3]) in the field. Hyperspectral sensors capture electromagnetic radiation reflected from vegetation in the visible (400–700 nm), near-infrared (700–1,300 nm), and short-wavelength infrared (1,400–3,000 nm) regions, which contain information about leaf physiological status, including pigments, structural constituents of biomass, and water content (Curran, 1989; Martin and Aber, 1997; Penuelas and Filella, 1998). Vegetation spectra can be captured in a few seconds, and universal indices have

[1] This work was supported by the National Science Foundation (grant no. PGR–1238030) and by a Fulbright Western Australia Scholarship (to T.T.).

* Address correspondence to lisa.ainsworth@ars.usda.gov.

The author responsible for distribution of materials integral to the findings presented in this article in accordance with the policy described in the Instructions for Authors (www.plantphysiol.org) is: Elizabeth A. Ainsworth (lisa.ainsworth@ars.usda.gov).

C.R.Y., E.A.A., P.J.B., L.M.M., and A.D.B.L. conceived of and designed the original research plans; C.R.Y., T.T., and C.M.M. performed most of the experiments; Y.C. provided technical assistance to C.R.Y.; C.R.Y., A.M.M., L.M.M., and E.A.A. analyzed the data; C.R.Y. and E.A.A. wrote the article with contributions from all of the authors.

[OPEN] Articles can be viewed without a subscription.

www.plantphysiol.org/cgi/doi/10.1104/pp.16.01447

been proposed to estimate leaf foliar traits such as chlorophyll content, nitrogen (N) content, and photosynthetic radiation use efficiency from reflectance data (Gamon et al., 1997; le Maire et al., 2004; Herrmann et al., 2010). Predictive models using partial-least squares regression (PLSR) approaches to scale spectral data also have been applied to estimate crop yield (Weber et al., 2012) and to estimate leaf features, including isotopic ratios (Richardson and Reeves, 2005), the ratio of leaf mass to leaf area (Asner and Martin, 2008; Asner et al., 2011), carbohydrate content of plant tissues (Dreccer et al., 2014; Asner and Martin, 2015), and the maximum photosynthetic capacity of C_3 plants (Serbin et al., 2012; Ainsworth et al., 2014). Variation in foliar reflectance at different wavelengths in the spectrum is specific to variation in different chemical and structural components of leaves (Curran, 1989; Serbin et al., 2014). Therefore, analysis of foliar reflectance spectra has the potential to very rapidly assess multiple physiological and biochemical traits from a single measurement.

The use of hyperspectral reflectance as a high-throughput phenotyping tool in agricultural research is promising (Weber et al., 2012; Araus and Cairns, 2014), but questions remain regarding limitations of the technique. Reflectance spectroscopy has been used to successfully distinguish broad-scale spatial and temporal variation in leaf foliar traits and photosynthetic metabolism across species in diverse agroecosystems (Serbin et al., 2015), tropical ecosystems (Asner and Martin, 2008; Asner et al., 2011), and northern temperate and boreal forests (Serbin et al., 2014). In this study, we test the utility of leaf hyperspectral reflectance as a high-throughput method for phenotyping diverse germplasm subject to abiotic stress in maize. Maize is one of the world's most important crops and also represents a model for species with C_4 photosynthesis. The relationship of hyperspectral reflectance with C_4 leaf traits has the potential to be distinct from that of C_3 species due to the significantly different leaf anatomy, biochemistry, and physiology of the two photosynthetic types.

We grew diverse maize genotypes in the field under ambient and elevated [O_3] using Free Air Concentration Enrichment (FACE). O_3 is an air pollutant that enters leaves through the stomata, where it rapidly forms other reactive oxygen species that cause damage to biochemical constituents and physiological processes, ultimately leading to reductions in leaf longevity and yield (Fiscus et al., 2005; Ainsworth et al., 2012). Past efforts to detect the genetic variation in O_3 tolerance using mapping populations have scored visible leaf damage or plant biomass (Kim et al., 2004; Frei et al., 2008; Brosché et al., 2010; Street et al., 2011; Ueda et al., 2015) but have not quantified the many other physiological changes that ultimately determine the impact of O_3 on crop yield. These include reduced photosynthetic capacity, reduced leaf chlorophyll and N content, accelerated senescence, increased antioxidant capacity, altered carbohydrate and metabolite content, decreased specific leaf area (SLA), and increased rates of respiration (Fiscus et al., 2005; Leitao et al., 2007; Dizengremel et al., 2008; Betzelberger et al., 2012; Gillespie et al., 2012). The logistics and cost of employing traditional phenotyping methods to quantify these physiological and biochemical markers of stress are prohibitive at the scale needed to screen large populations, so hyperspectral reflectance offers a promising nondestructive, rapid, and high-throughput alternative. However, this alternative approach has yet to be validated.

In order to test the throughput of this approach in the field, we collected reflectance spectra from diverse inbred and hybrid maize lines grown in ambient and elevated [O_3] in replicated plots across a 16-ha field over three consecutive growing seasons as well as greenhouse-grown maize (inbred B73) given optimal and limiting N supply. This range of conditions and material was developed to ensure that a wide range of values were measured. These same leaves were sampled using gold standard techniques of gas-exchange and wet-laboratory biochemical approaches to quantify traits relevant to leaf stress physiology, including chlorophyll content, N content, SLA, maximum rate of phospho*enol*pyruvate carboxylation ($V_{p,max}$), [CO_2]-saturated rate of photosynthesis (V_{max}), leaf oxygen radical absorbance capacity (ORAC), and Suc content. The two data sets were used successfully to build predictive PLSR models for five of seven traits and to demonstrate that similar conclusions about genetic and treatment variation in leaf traits were drawn from both measured and modeled data.

RESULTS

Predicting Physiological Traits from Reflectance Spectra

PLSR models using the leave-one-out cross-validation approach predicted leaf biochemical and physiological traits with varying degrees of accuracy. The predictive ability was strongest for chlorophyll (r^2 = 0.81–0.85; Fig. 1, A and B) and N content (r^2 = 0.92–0.96; Fig. 1, C and D), good for SLA (r^2 = 0.68–0.78; Fig. 1, E and F), V_{max} (r^2 = 0.56–0.65; Fig. 1, G and H), and Suc content (r^2 = 0.62; Fig. 2A), and nonsignificant for $V_{p,max}$ (Fig. 1, I and J) and ORAC (Fig. 2B). In general, models created with spectra collected from leaves exposed to multiple growth environments (i.e. greenhouse and field, low and high N, and ambient and elevated [O_3]) captured a greater proportion of trait variation than models built from just field-grown plants. For example, a stronger correlation between measured and model-predicted chlorophyll values was observed with the combined field and greenhouse model (r^2 = 0.85; Fig. 1B) compared with the field-only model (r^2 = 0.81; Fig. 1A). Similarly, the correlations for N content and V_{max} were stronger using both greenhouse and field data. In contrast, inclusion of data from greenhouse-grown maize plants did not improve the SLA model (Fig. 1F). No greenhouse samples were collected for ORAC and Suc quantification; therefore, models consisted only of data from the field (Fig. 2). PLSR model coefficients for each trait are provided in Supplemental Table S1.

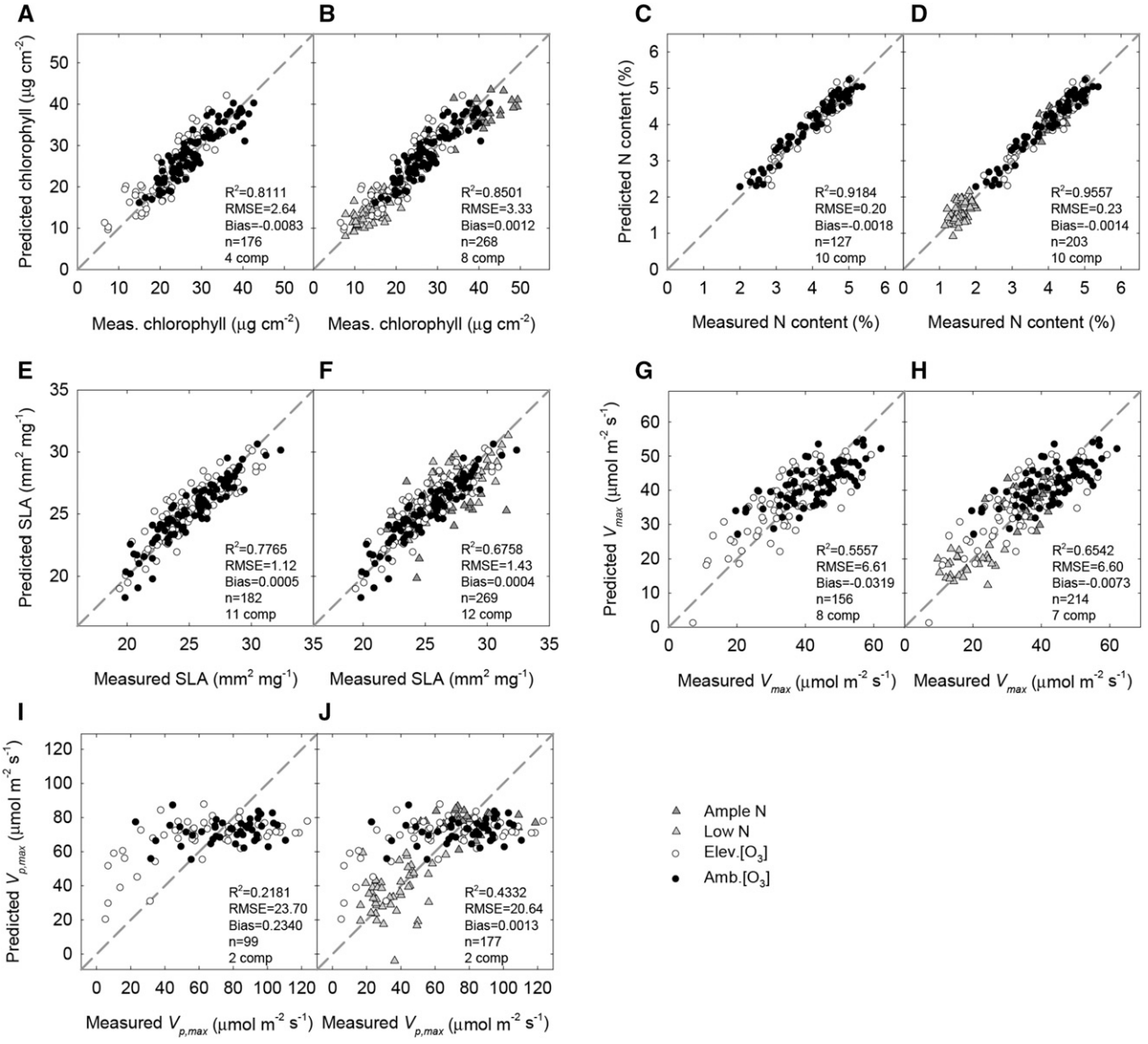

Figure 1. Measured versus PLSR-modeled values of leaf chlorophyll content (A and B), N content (C and D), SLA (E and F), V_{max} (G and H), and $V_{p,max}$ (I and J). PLSR models were built using a training population consisting of genotypically diverse field-grown plants exposed to ambient and elevated [O_3] (A, C, E, G, I) or a combination of field-grown plants and greenhouse plants (genotype B73) grown in ample or limiting N (B, D, F, H, J). In each graph, the cross-validation r^2, root mean square error (RMSE), and bias of the model are shown along with the size of the validation population and the number of model components (comp) used in each PLSR model. The gray dashed line shows the 1:1 line.

As an additional test of PLSR model stability, 20% of the measured values used for training the original PLSR models were randomly selected and removed (as a holdout data set). A second set of PLSR models was built using the remaining 80% of the original training data (80% model). The parameter estimates generated by the 80% model were very similar to the parameter estimates from the original, full model (Supplemental Table S2). In addition, the 80% model accurately estimated the measured values of the holdout data set that were removed prior to model building (Supplemental Table S2).

In order to test the similarity in relationships among traits for measured and PLSR-modeled data, pairwise correlations among traits were examined (Fig. 3). In both measured and PLSR-modeled data sets, the correlations were consistent, demonstrating that the relationships among the underlying measured traits were accurately reflected by the PLSR models. N content and V_{max} were positively correlated, and there were significant correlations between chlorophyll content and N content and V_{max} (Fig. 3). N content was negatively correlated to Suc content, and chlorophyll content was negatively correlated to SLA (Fig. 3).

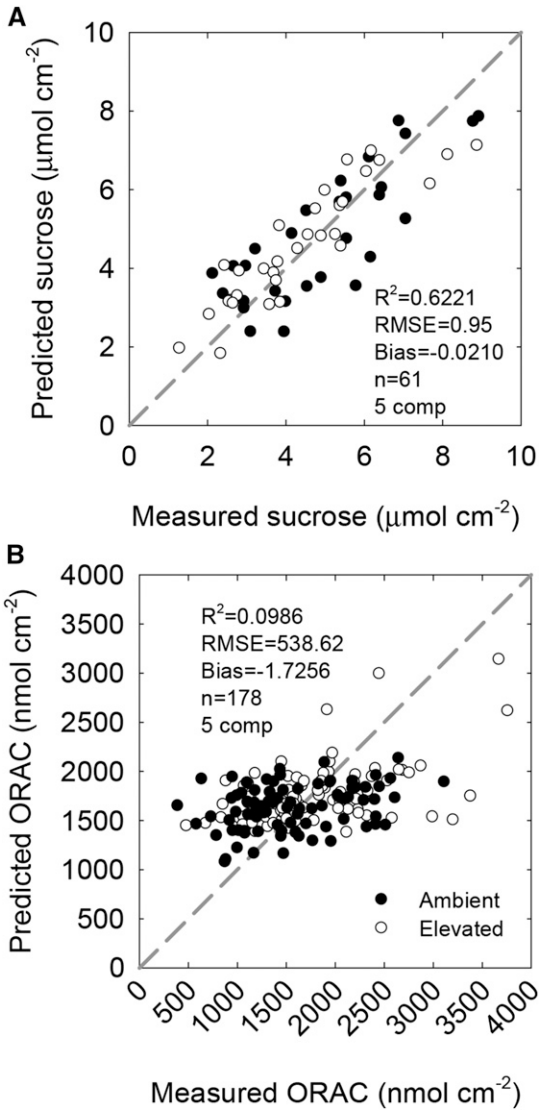

Figure 2. Measured PLSR-modeled values of leaf Suc content (A) and leaf total ORAC (B). PLSR models were built using a training population consisting of diverse field-grown maize inbred and hybrid lines exposed to ambient and elevated [O_3]. In each graph, the cross-validation r^2, RMSE, and bias of the model are shown along with the size of the validation population and number of model components (comp) used in each PLSR model. The gray dashed line shows the 1:1 line.

PLSR models were able to distinguish the same effects as measured traits. Using genotypes B73, Mo17, and the B73 × Mo17 hybrid, ANOVA models estimating the effects of genotype, O_3 treatment, and the interaction had consistent inferences for three of four successful PLSR models (chlorophyll, N, and V_{max}; Supplemental Table S3; Supplemental Fig. S1). For SLA, the P value for the O_3 effect on measured data was 0.012 and the P value for the PLSR-modeled data was 0.095 (Supplemental Table S3).

To assess the relative contributions of different wavelengths across the measured spectra as drivers of a given PLSR model, variable importance in projection (VIP) scores for each trait model were compared. The chlorophyll model was very sensitive to variation in reflection of visible wavelengths, with major peaks at 554 and 719 nm and minor contributions from the short-wavelength infrared region (Fig. 4A). The N content model was built with wavelengths between 1,500 and 2,400 nm based on the dominant absorption features of N (Curran, 1989; Serbin et al., 2014) and was sensitive to variation in reflectance throughout that region of the spectrum. The SLA (Fig. 4B) and Suc content (Fig. 4C) models both had influential peaks in the visible wavelengths that overlapped with the chlorophyll model but also showed trait-specific contributions throughout the near- and short-wavelength infrared regions. The chlorophyll and V_{max} models were very similar in the visible portion of the spectrum, with moderate differences between 800 and 1,750 nm (Fig. 4D).

As an alternative to PLSR model building, chlorophyll, N, and SLA also were estimated using previously published simple indices and correlated with direct measures of traits (Table I). Several indices, including mNDVI, mSR_{CHL}, SIPI, and SR2, were unable to predict chlorophyll content accurately in maize leaves (r^2 = 0.064, 0.006, 0.067, and 0.172). Estimated chlorophyll values from other indices were correlated with measured values (Table I), but even the best of these indices, based on the coefficient of determination (Datt4; r^2 = 0.74), was outperformed by the PLSR model (r^2 = 0.85; Fig. 1B). Trait values estimated using previously published indices for N content and SLA showed poor correlations with measured values and were outperformed by PLSR analysis of reflectance spectra (Table I; Fig. 1).

High-Throughput Screening of Diverse Inbred and Hybrid Maize for O_3 Response

Once it was determined that PLSR models could reasonably predict foliar biochemical and physiological traits, we tested the approach for high-throughput phenotyping potential by screening diverse inbred and hybrid maize lines grown in the field at ambient and elevated [O_3] in 2013, 2014, and 2015 (Supplemental Table S4). Using two spectroradiometers, we were able to collect leaf reflectance spectra from maize plants grown in 1,024 rows spread across a 16-ha field in 2 to 4 d while limiting the period of measurement to the middle 4 h of each day (approximately 11 AM to 3 PM). By contrast, destructive sampling from each of the rows of the experiment required 12 people to sample for 4 to 5 h over 2 d, making sample collection approximately 6 times more efficient for spectral traits. The time savings of spectral reflectance over wet chemistry were even more dramatic for postprocessing of samples and data. Analysis of spectral data took approximately 10 d, while processing and analysis of samples for wet chemistry and leaf gas exchange took between 30 and 90 d depending on the trait.

Diverse inbred and hybrid maize genotypes showed a 1.3- to 2.2-fold range of values for chlorophyll content, N content, SLA, Suc content, and V_{max}, as estimated by the PLSR models (Fig. 5). For example, in 2014,

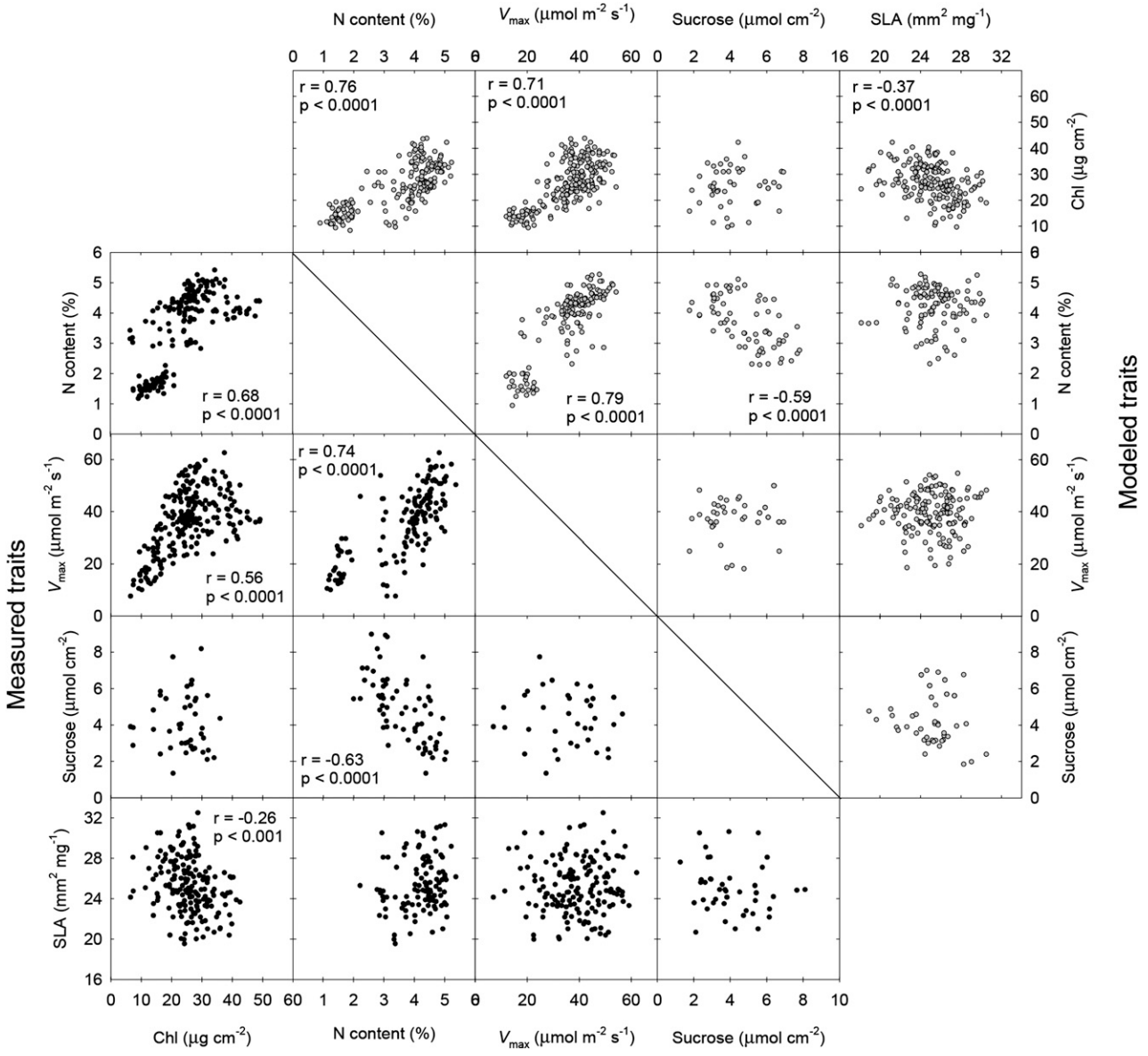

Figure 3. Pairwise correlations of measured (black symbols) and modeled (gray symbols) leaf traits. Modeled traits are partial least-squares predictions from leaf reflectance spectra collected from diverse maize inbred and hybrid lines. Chl, Chlorophyll.

chlorophyll content ranged from 15.2 to 31.2 μg cm^{-2} (Fig. 5A), N content from 3.2% to 4.3% (Fig. 5B), SLA from 20.6 to 29.6 mm^2 mg^{-1} (Fig. 5C), Suc content from 3.8 to 5.7 μmol cm^{-2} (Fig. 5D), and V_{max} from 18.8 to 41.1 μmol m^{-2} s^{-1} (Fig. 5E) in the 52 inbred genotypes grown at ambient [O_3]. In general, the range of trait values for hybrids grown in ambient [O_3] was narrower than for inbreds grown at ambient [O_3] (Fig. 5), as may be expected because all of the hybrids shared a common parent in B73 (Supplemental Table S4). Hybrid genotypes also had greater average chlorophyll, N, and V_{max} compared with inbred genotypes and lower average Suc content (Fig. 5D). Inbred and hybrid genotypes grown at elevated [O_3] showed significant reductions in chlorophyll content in all years (Fig. 5A; Table II), and while there was some interannual variation, elevated [O_3] also decreased N content and V_{max} (Fig. 5, B and E; Table II) and increased SLA (Fig. 5C; Table II).

DISCUSSION

This study demonstrates the ability to rapidly and cost-effectively screen for intraspecific variation in maize leaf biochemical and physiological traits using PLSR models applied to leaf reflectance spectra. Leaf chlorophyll content, N content, SLA, Suc content, and V_{max} could be predicted from reflectance spectra of maize (Figs. 1 and 2). This capability to rapidly and simultaneously capture five of the most commonly assessed and important leaf traits to plant carbon and N

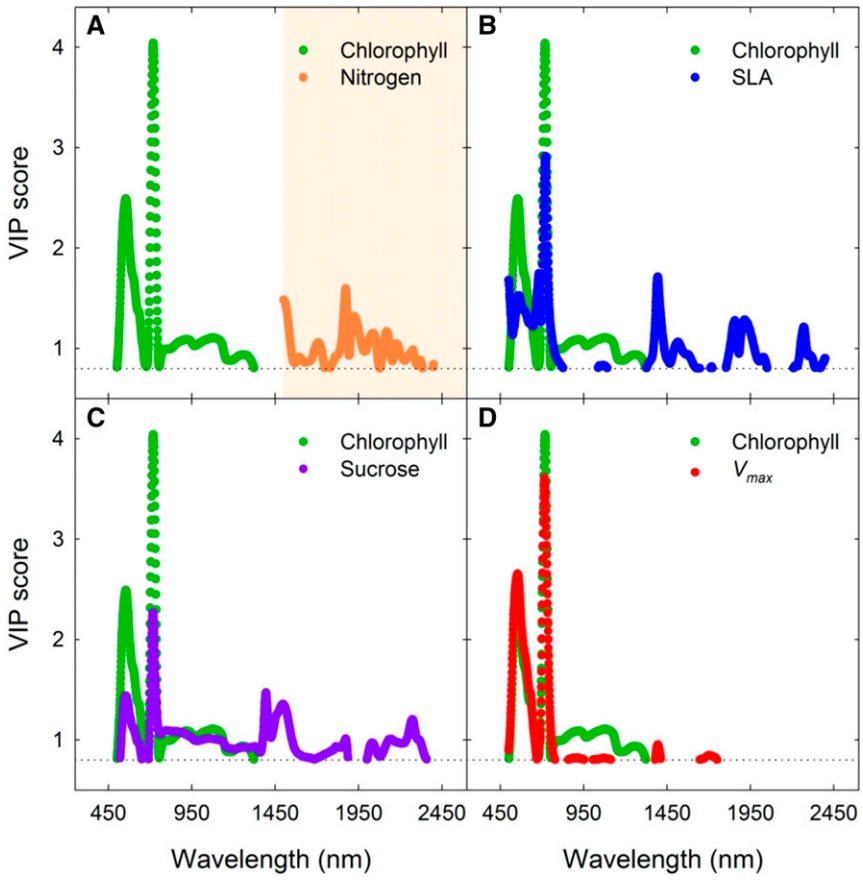

Figure 4. VIP across the spectral region for each PLSR model. VIP scores for the chlorophyll model are compared with models for N content (%; A), SLA (B), Suc (C), and V_{max} (D). A VIP score greater than 0.8 is considered to influence the trait estimate (Wold, 1994). The orange shaded area in A indicates that the model for N content was built using a truncated spectral region (1,500–2,400 nm). All other models utilized the spectrum from 500 to 2,400 nm.

relations in a single spectrum represents a significant advance with a wide range of potential applications in maize genetics and breeding. Previous attempts to use remote sensing to investigate O_3 damage in maize measured visual damage to leaves and canopies (Runeckles and Resh, 1975; Kraft et al., 1996; Rudorff et al., 1996; for review, see Meroni et al., 2009), most often in terms of the normalized difference vegetation index, which is based on differences in surface reflectance in the near-infrared and visible ranges of the spectrum. This was also limited to canopy-level remote sensing of a single maize genotype. This study demonstrated success in the early detection and evaluation of leaf-level biochemical and physiological responses when visual symptoms of O_3 stress were minimal. The proof of concept for the use of spectral reflectance to detect phenotypic variation within a C_4 species is a significant advance over previous uses of similar techniques that have distinguished larger species-level differences in natural or agricultural ecosystems (Asner and Martin, 2008; Asner et al., 2011; Serbin et al., 2012, 2014, 2015).

High-Throughput Phenotyping with Hyperspectral Reflectance

High-throughput field phenotyping efforts have successfully investigated morphological, developmental, and agronomic traits in large numbers of crop genotypes. However, rapid measurements of physiological traits are needed to fully understand plant-environment interactions, including the plant stress response (Großkinsky et al., 2015). For field phenotyping to be maximally useful, approaches should be high throughput, precise, and multidimensional, providing accurate information about relevant traits (Dhondt et al., 2013). The hyperspectral reflectance and PLSR modeling approach taken in this study meets those goals. The collection of leaf reflectance spectra takes less than 1 min per leaf and is nondestructive, so it is possible to monitor a leaf over its lifetime. To estimate V_{max} from gas exchange, it could take at least 20 to 30 min to assess the response of net assimilation (A) to variation in intercellular [CO_2] (C_i) curve on a single leaf. Even measurements of maximum light and CO_2-saturated photosynthesis could take 5 to 10 min per leaf in the field, where the leaf has to acclimate to the cuvette conditions, which may differ from atmospheric conditions. Generating parameter estimates by fitting a photosynthesis model to the measured gas-exchange data would take approximately the same amount of time as fitting the PLSR model. Therefore, we estimate that the reflectance approach for estimating V_{max} is at least 10 times faster in terms of data collection and can be completed during a shorter period of time during the day to avoid circadian or diurnal effects on leaf traits that might confound measurements taken over a longer

Table I. *Estimates of chlorophyll content,* N *content, and* SLA *calculated using published spectral indices and compared with measured values*

Each index was applied to the same spectra used for the PLSR model training population. For each index, the predictive formula is shown along with the correlation coefficient, RMSE, and reference.

Trait	Index	Formulation	Adjusted r^2	RMSE	Reference
Chlorophyll	Datt4	$R_{672}/(R_{550} \times R_{708})$	0.740	3.23	Datt (1998)
	Vogelmann2	$(R_{734} - R_{747}) - (R_{715} + R_{726})$	0.736	3.26	Vogelmann et al. (1993)
	Maccioni	$(R_{780} - R_{710})/(R_{780} - R_{680})$	0.714	3.39	Maccioni et al. (2001)
	Double Difference	$(R_{749} - R_{720}) - (R_{701} - R_{672})$	0.702	3.46	le Maire et al. (2004)
	Vogelmann1	R_{740}/R_{720}	0.701	3.47	Vogelmann et al. (1993)
	mSR_{705}	$(R_{750} - R_{445})/(R_{705} - R_{445})$	0.680	3.58	Sims and Gamon (2002)
	$mNDVI_{705}$	$(R_{750} - R_{705})/(R_{750} + R_{705} - 2R_{445})$	0.653	3.73	Sims and Gamon (2002)
	SR3	R_{750}/R_{550}	0.580	4.11	Gitelson and Merzlyak (1997)
	SR4	R_{700}/R_{670}	0.498	4.49	McMurtey et al. (1994)
	SR1	R_{750}/R_{700}	0.457	4.67	Gitelson and Merzlyak (1997)
	Gitelson	$1/R_{700}$	0.387	4.96	Gitelson et al. (1999)
	SR2	R_{752}/R_{690}	0.172	5.77	Gitelson and Merzlyak (1997)
	SIPI	$(R_{800} - R_{445})/(R_{800} - R_{680})$	0.067	6.12	Penuelas et al. (1995)
	mNDVI	$(R_{800} - R_{680})/(R_{800} + R_{680} - 2R_{445})$	0.064	6.13	Sims and Gamon (2002)
	mSR_{CHL}	$(R_{800} - R_{445})/(R_{680} - R_{445})$	0.006	6.36	Sims and Gamon (2002)
N	NRI_{1510}	$(R_{1510} - R_{660})/(R_{1510} + R_{660})$	0.450	0.90	Herrmann et al. (2010)
	$MCARI_{1510}$	$[(R_{700} - R_{1510}) - 0.2(R_{700} - R_{550})] \times (R_{700}/R_{1510})$	0.239	1.05	Herrmann et al. (2010)
	NDNI	$[\log_{10}(1/R_{1510}) - \log_{10}(1/R_{1680})]/[\log_{10}(1/R_{1510}) + \log_{10}(1/R_{1680})]$	0.198	1.08	Serrano et al. (2002)
SLA	mND	$(R_{2285} - R_{1335})/[R_{2285} + R_{1335} - (2 \times R_{2400})]$	0.177	2.43	le Maire et al. (2008)
	NDMI	$(R_{1649} - R_{1722})/(R_{1649} + R_{1722})$	0.133	2.49	Cheng et al. (2014)
	ND_{LMA}	$(R_{1368} - R_{1722})/(R_{1368} + R_{1722})$	0.122	2.51	Cheng et al. (2014)
	mSR_{SLA}	$(R_{2265} - R_{2400})/(R_{1620} - R_{2400})$	0.073	2.58	le Maire et al. (2008)
	SR	R_{2295}/R_{1500}	0.070	2.58	le Maire et al. (2008)
	ND	$(R_{1710} - R_{1340})/(R_{1710} + R_{1340})$	0.061	2.60	le Maire et al. (2008)

period of time (Dodd et al., 2005). For other traits, like Suc content or N content, gold standard measurements require a destructive leaf sample for biochemical analysis, which is lower throughput and does not allow repeated monitoring over time. Estimation of numerous traits from a single spectrum provides multidimensionality, and the speed with which spectra can be collected means that, at least temporally, measurements can be taken with high resolution. In this study, we derived leaf-level biochemical and structural traits from leaf reflectance spectra collected with a leaf clip that provided a uniform light environment, thus minimizing some of the environmental and spatial variation that canopy-level reflectance measurements inevitably have. The leaf clip facilitates the investigation of tissue-level phenomena and the effects of leaf age, but there is a tradeoff in that further study would be needed to scale these leaf-level parameters to a canopy.

Leaf-Level Predictive Models

Leaf-level hyperspectral data have been used previously to estimate photosynthetic parameters in C_3 species (Doughty et al., 2011; Serbin et al., 2012) but not in C_4 species, which have a carbon-concentrating mechanism and different biochemical limitations to photosynthetic rate than C_3 species. For example, while light-saturated photosynthetic rate is limited by carboxylation capacity at low intercellular [CO_2] in C_3 plants (Farquhar et al., 1980), it is instead limited by phospho*enol*pyruvate carboxylase activity at low intercellular [CO_2] in C_4 plants (von Caemmerer, 2000). C_3 and C_4 species also invest differentially in photosynthetic proteins and pigments and have leaves with distinct morphological and structural characteristics. Based on these differences, a number of studies have used remote sensing approaches to distinguish C_3 and C_4 species experimentally or on the landscape (Irisarri et al., 2009; Liu and Cheng, 2011; Adjorlolo et al., 2012). Perhaps it is not surprising that a new PLSR model was needed to estimate parameters related to C_4 photosynthesis in maize, especially given that predictions of photosynthetic capacity are not direct expressions of the reflectance spectra but, instead, are due to a combination of anatomical (e.g. SLA) and chemical (e.g. N or chlorophyll) factors that are expressed more directly in reflectance spectra (Jacquemoud and Baret, 1990). In our study, we could not use reflectance spectra to accurately predict $V_{p,max}$ in maize (Fig. 1, I and J) but could accurately predict V_{max} (Fig. 1, G and H). It will be interesting to test if this is also the case for other C_4 species.

Similar to previous PLSR models for C_3 photosynthetic parameters (Serbin et al., 2012), the C_4 PLSR model for V_{max} used wavebands in the visible region of the spectrum where chlorophyll and other pigments have strong features but also used wavebands in the

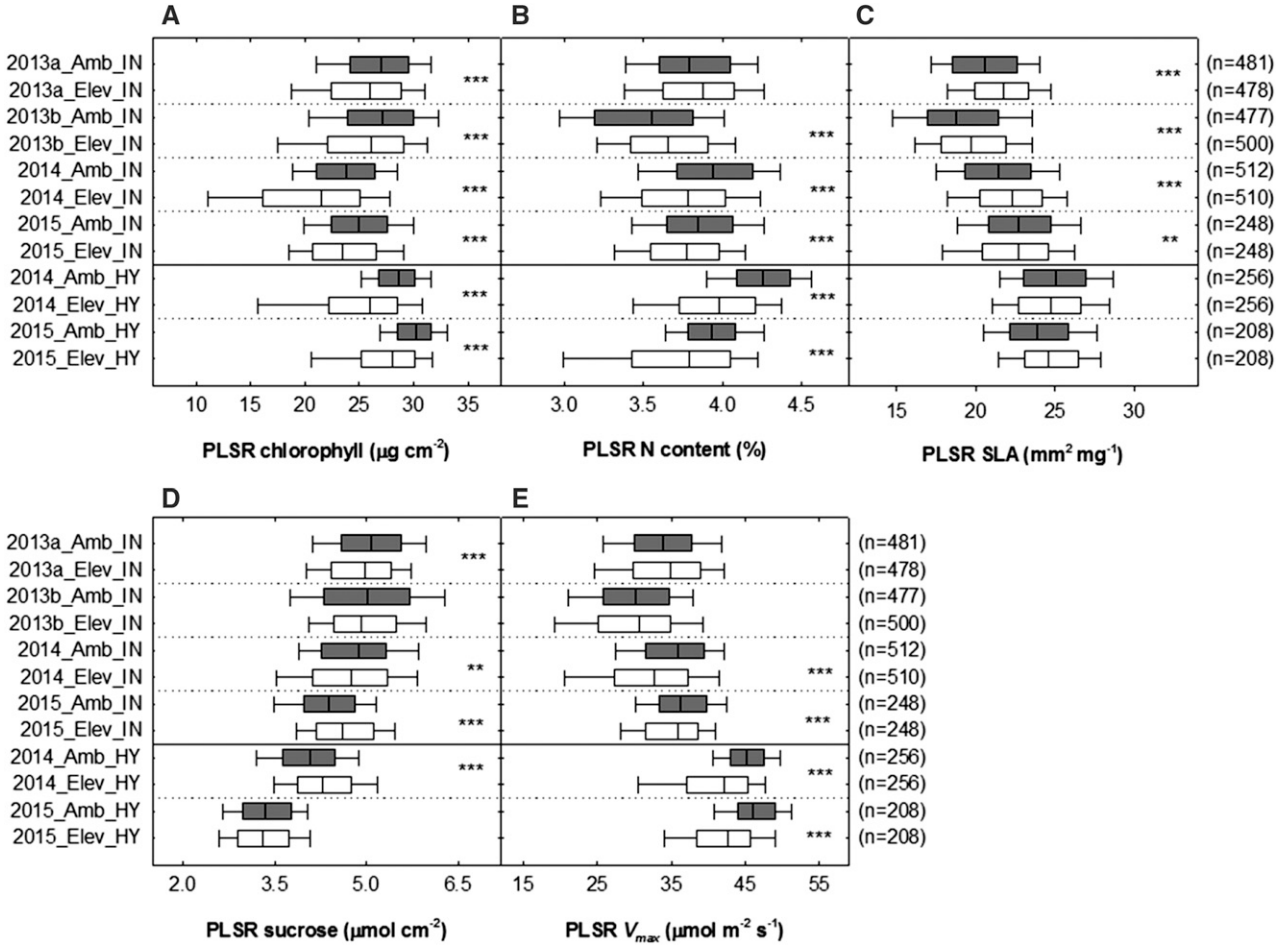

Figure 5. Box plots showing the distribution of values estimated from PLSR models for diverse maize genotypes, including foliar chlorophyll content (A), N content (B), SLA (C), Suc content (D), and V_{max} (E). Maize inbred (IN) and hybrid (HY) genotypes were grown at ambient (Amb; approximately 40 nL L^{-1}) and elevated (Elev; 100 nL L^{-1}) [O_3] in each of the three growing seasons. Spectra were collected from July 14 to 17, 2013 (2013a), July 29 to 30, 2013 (2013b), July 14 to 18, 2014, and July 15 to 16, 2015. The number of individual rows sampled successfully during each time point is shown in parentheses. Asterisks indicate significant effects of elevated [O_3] within a given time point: **, $P < 0.01$; and ***, $P < 0.001$.

near-infrared and short-wavelength infrared regions (Fig. 4), indicating that V_{max} is not simply a function of chlorophyll content. We also observed, along with previous studies (Hansen and Schjoerring, 2003; Doughty et al., 2011; Serbin et al., 2012), that both the measured and PLSR-modeled leaf traits were significantly correlated (Fig. 3). Relationships among leaf structural and biochemical traits also converge across a very diverse range of species, and photosynthesis is positively correlated to leaf N content and SLA (Reich et al., 1997; Wright et al., 2004). Global trait databases also have reported correlations between leaf N content and SLA (Reich et al., 1997); however, this correlation was not significant within diverse maize lines (Fig. 3). This may be because within-species variation is more constrained than across-species variation in leaf traits. Most importantly, the same conclusions about correlation among traits and variation in leaf traits due to genotype or treatment were drawn from tests of measured and modeled data (Fig. 3; Supplemental Fig. S1; Supplemental Table S3).

PLSR models developed for maize also improved predictions of chlorophyll content, N content, and SLA compared with previously published simple indices (Table I). The performance improvement of the PLSR model compared with simple indices has been reported previously (Hansen and Schjoerring, 2003; Atzberger et al., 2010) and has several contributing sources. First, PLSR takes advantage of the full spectral information, most of which is excluded by simple indices, yet clearly contributes to improved trait prediction based on underlying biophysical or biochemical attributes (Hansen and Schjoerring, 2003). PLSR also is relatively insensitive to sensor noise (Atzberger et al., 2010). The other advantage is in building models specifically to the species under study, in this case maize, while the other simple indices were built using other species or diverse species (Vogelmann et al., 1993; Datt, 1998; Maccioni et al., 2001;

Table II. *Statistical analysis (P values) of the effects of elevated [O_3], genotype (Gen), and the interaction of [O_3] and genotype on leaf physiological and biochemical traits estimated from leaf reflectance spectra*

Box plots of leaf traits are shown in Figure 5. Spectra were collected from July 14 to 17, 2013 (2013a), July 29 to 30, 2013 (2013b), July 14 to 18, 2014 (2014), and July 15 to 16, 2015 (2015). Inbred and hybrid lines were evaluated in different statistical models.

Parameter	Chlorophyll	N	V_{max}	SLA	Suc
Inbred lines					
2013a					
[O_3]	<0.0001	0.17	0.56	<0.0001	<0.0001
Gen	<0.0001	<0.0001	<0.0001	<0.0001	<0.0001
[O_3] × Gen	0.19	0.60	0.05	0.94	0.12
2013b					
[O_3]	<0.0001	<0.0001	0.95	<0.0001	0.05
Gen	<0.0001	<0.0001	<0.0001	<0.0001	<0.0001
[O_3] × Gen	0.90	0.35	0.72	0.98	0.99
2014					
[O_3]	<0.0001	<0.0001	<0.0001	<0.0001	0.004
Gen	<0.0001	<0.0001	<0.0001	<0.0001	<0.0001
[O_3] × Gen	0.0002	0.05	0.03	<0.0001	<0.0001
2015					
[O_3]	<0.0001	<0.0001	0.0007	0.01	<0.0001
Gen	<0.0001	<0.0001	<0.0001	<0.0001	<0.0001
[O_3] × Gen	0.17	0.32	0.42	0.05	0.25
Hybrid lines					
2014					
[O_3]	<0.0001	<0.0001	<0.0001	0.08	<0.0001
Gen	0.0005	0.12	0.0008	<0.0001	<0.0001
[O_3] × Gen	0.07	0.40	0.22	0.86	0.29
2015					
[O_3]	<0.0001	0.68	<0.0001	0.0007	<0.0001
Gen	<0.0001	<0.0001	<0.0001	0.004	0.02
[O_3] × Gen	0.74	0.90	0.33	0.74	0.75

le Maire et al., 2004, 2008). Of course, this may be a disadvantage as well, and further studies need to test whether the PLSR models developed for maize in this study also can be accurately used in other C_4 species.

High-Throughput Phenotyping of the Stress Response in Maize

This study used diverse maize lines grown at elevated [O_3] as a proof-of-concept test bed for high-throughput phenotyping of leaf biochemical traits using leaf reflectance spectra. The maize inbred lines represent much of the genetic diversity within the species (McMullen et al., 2009), and elevated [O_3], as a treatment, provides an attractive test for this approach environment because common phenotypes associated with O_3 damage include reduced photosynthetic capacity, leaf N content, and chlorophyll content, increased respiration rates and levels of antioxidants, and altered SLA (Reich and Amundson, 1985; Fiscus et al., 2005; Betzelberger et al., 2012). Based on the biochemical and physiological traits estimated from hyperspectral reflectance, both maize inbreds and hybrids were sensitive to elevated [O_3] and showed reduced chlorophyll, N content, and photosynthetic capacity (Fig. 5; Table II). This was accompanied by greater SLA, indicating reduced leaf mass per unit area, which often is associated with lower photosynthetic capacity and/or lower starch content (Poorter et al., 2012). This is consistent with the accelerated leaf senescence at elevated [O_3] observed in other species (Miller et al., 1999; Ainsworth et al., 2012; Gillespie et al., 2012) and with reduced carbon gain being at least partly responsible for the 10% reduction in yield of U.S. maize due to O_3 over the last 30 years (McGrath et al., 2015). This study also showed that, using hyperspectral reflectance, it was possible to detect genotypic differences in physiological and biochemical leaf traits across maize lines and variation in their response to elevated [O_3] (Fig. 5). The ability to rapidly detect this variation in the field across a diverse panel of genotypes is a key first step to improving abiotic stress tolerance in maize.

CONCLUSION

Rapid measurement of physiological traits is widely anticipated as a transformative technology for the experimental research needed to understand the mechanisms of crop stress response and to maximize the advantage of genetic resources for crop improvement. Here, we provide evidence that leaf-level physiological and biochemical traits that are hallmark markers of stress response can be accurately predicted from PLSR models built from leaf reflectance spectra in maize,

thereby providing a high-throughput, nondestructive method for phenotyping.

MATERIALS AND METHODS

Greenhouse Experiment

Maize (*Zea mays*) genotype B73 was planted on March 15, 2014, in 17-cm-diameter pots containing potting mix (Sunshine LC1 mix; Sun Gro Horticulture). Plants were grown in the greenhouse and fertilized with 40% Long Ashton nutrient solution (Hewitt and Smith, 1975) with either 6 mM NH_4NO_3 (ample N) or 0.25 mM NH_4NO_3 (low N) starting 20 d after planting. The greenhouse was sunlit, and additional supplemental lighting from metal halide lamps provided a minimum photosynthetic photon flux density of 200 μmol m^{-2} s^{-1} from 6 AM to 8 PM. Foliar tissue and hyperspectral measurements were collected 55 to 60 d after planting from a developmental range of leaves at V7 to V10.

Field Experiments

Diverse inbred and hybrid maize genotypes (Supplemental Table S4) were grown in ambient and elevated [O_3] at the Free Air Concentration Enrichment field site in Champaign, Illinois (soyface.illinois.edu) during the growing seasons of 2013, 2014, and 2015. Maize genotypes were planted with a precision planter in 3.35-m rows at a density of eight plants per meter and row spacing of 0.76 m. In 2013, 203 inbred genotypes were grown at ambient and elevated [O_3] (n = 2) in octagonal rings approximately 20 m in diameter. Each individual genotype was planted in a single row plot within a ring. Placement of individual genotypes was randomized between the two replicates, and the location of each genotype was fixed within a pair of ambient and elevated [O_3] rings (ring pair) that were located near one another in the field (but still separated by approximately 100 m). B73 was planted in 12 locations within each ring in 2013. In 2014, 52 inbred and 26 hybrid genotypes were grown at ambient and elevated [O_3] (n = 4). Each inbred genotype was planted in a single row within each ring, and the location of genotypes was randomized among the four replicates but conserved within an ambient and elevated [O_3] ring pair. Each hybrid genotype was planted in two rows within each ring and randomized as described above for inbred genotypes. In 2014, B73 was planted in 10 rows within each inbred ring and B73 × Mo17 was planted in 14 rows within each hybrid ring. In 2015, 10 inbred and eight hybrid genotypes were grown at ambient and elevated [O_3] (n = 4). Each genotype was planted in five rows within each octagonal ring with a spatial design ensuring that each genotype was planted in one row in the central, north, south, east, and west sides of the ring.

O_3 was increased to a target set point of 100 nL L^{-1} from approximately 10 AM to 6 PM throughout the growing seasons using free-air O_3 enrichment technology, as described by Morgan et al. (2004) with the following modifications. O_3 was produced by passing high voltage through oxygen in O_3 generators (CFS-3 2G; Ozonia) and then added to compressed air for fumigation. O_3-enriched air was released on the upwind sides of the octagon from horizontal pipes surrounding the rings. Within each ring, there was a 1-m buffer area that was not used for experiments. Fumigation was stopped when leaves were wet (during rain) and when wind speed was too low (less than 0.5 m s^{-1}) to maintain consistent treatment. The average daily [O_3] and cumulative [O_3] exposures during the 2013, 2014, and 2015 growing seasons are summarized in Supplemental Table S5.

Training Data Set

Training data sets were collected to pair leaf reflectance spectra with gold standard biochemical and physiological measurements of chlorophyll content, N content, SLA, V_{max}, $V_{p,max}$, Suc content, and ORAC. Measurements for the training data set were collected from diverse maize lines grown at ambient and elevated [O_3] in the field in 2014 and 2015 and from inbred line B73 grown in the greenhouse at high and low N availability. The training data sets for each of the successful PLSR traits are provided in Supplemental Data Set S1.

Gold Standard Methods for Measuring Leaf Physiology and Biochemistry

To determine $V_{p,max}$ and V_{max} for the training data set, the response of A to C_i was measured across a range of [CO_2] from 25 to 1,500 μmol mol^{-1} using a portable photosynthesis system (LI-6400; LICOR Biosciences) set at constant photosynthetic photon flux density (2,000 μmol m^{-2} s^{-1}). The approximately six initial points of the A/C_i curve ($C_i < 60$ μmol mol^{-1}) were fit to a model for phospho*enol*pyruvate carboxylase-limited photosynthesis (von Caemmerer, 2000) and used to estimated $V_{p,max}$. V_{max} was estimated as the horizontal asymptote of a four-parameter nonrectangular hyperbolic function (Markelz et al., 2011). Before starting each A/C_i curve, leaf temperature was measured with an infrared thermometer (62 MAX; Fluke) and used to set the leaf chamber cuvette at ambient conditions. This also ensured that gas-exchange measurements were done at the same temperature as leaf reflectance spectra. For the greenhouse experiment, two intact leaves were measured per plant: the first and third youngest leaf with a visible collar. For field samples, the third youngest leaf with a visible collar was excised and immediately recut under water prior to dawn.

Immediately after each A/C_i curve was completed, tissue was removed from the leaf using a cork borer and flash frozen in liquid N. One leaf disc (approximately 1.4 cm^2) was incubated in 96% (v/v) ethanol for 3 d at 4°C in order to determine chlorophyll content using the equations of Lichtenthaler and Wellburn (1983). Another leaf disc was used to determine the ORAC content following the procedures described by Gillespie et al. (2007). A third leaf disc was used to determine Suc content according to the methods of Jones et al. (1977). SLA was determined by weighing a known area of leaf tissue after drying for 5 d at 60°C. The dried leaf tissue was then ground to a fine powder and combusted with oxygen in an elemental analyzer (Costech 4010; Costech Analytical Technologies). N content was determined by comparing experimental samples with an acetanalide standard curve.

Maize Leaf Reflectance Spectroscopy

Before destructively sampling leaf tissue, reflectance spectra were captured from the adaxial surface of the same leaves that were used for gold standard measures of leaf physiology and biochemistry using a full-range spectroradiometer (ASD FieldSpec 4 Standard Res; Analytical Spectral Devices) equipped with an illuminated leaf clip contact probe. The scanning time for the instrument is approximately 100 ms, and each spectrum collected was the average of 10 scans. A reflective white reference (Spectralon; Labsphere) was used to standardize the relative reflectance of the samples. The spectroradiometer was turned on for at least 30 to 60 min before reflectance measurements began to allow for the three arrays to warm up. Reflectance measurements were obtained from the same location on the leaf as the A/C_i curve measurements and were restricted to the central section of the leaf, avoiding the midrib. A preliminary test calculated bootstrapped (100-fold) mean and variance values from a population of 25 measurements collected from a single leaf, from which we determined that six measurements per leaf reduced sample variance by over 50% (Supplemental Fig. S2). Subsequently, all leaf reflectance measurements used the average of six spectra from each leaf taken at different locations within an approximately 7-cm band in the central section of the leaf. Before averaging the six spectra collected from a single leaf, a splice correction was applied to the spectral observations to ensure continuous data across detectors. Data were interpolated to provide 1-nm bandwidths, and quality control was applied using the FieldSpectra package in R (Serbin et al., 2014).

PLSR Models

PLSR was used to develop predictive models with the open-source PLS package (Mevik and Wehrens, 2007) in R following the methods of Serbin et al. (2014). This approach identifies latent factors, or components, that account for most of the variation in a trait variable and generates a linear model consisting of waveband scaling coefficients to transform full-spectrum data. To maximize the predictive ability of the model while minimizing the possibility of overfitting, the predicted residual sum of squares (PRESS) statistic was used to determine the optimal number of model components (Chen et al., 2004). The number of components that minimized the RMSE of the PRESS statistic was chosen (Wold et al., 2001). We calculated the PRESS statistic through a leave-one-out cross-validation approach, which trains the model on all but one observation and then makes a prediction for the left-out observation. The average error is then computed and used to evaluate the model (Siegmann and Jarmer, 2015). VIP scores (Wold, 1994) also were determined to compare the relative significance of each wavelength in its contribution to the final model. The spectrum range for all models was 500 to 2,400 nm, except N content, which was restricted to 1,500 to 2,400 nm because of well-known attributes of N absorption (Curran, 1989; Serbin et al., 2014). Performance parameters were generated to assess the predictive ability of each model, including the coefficient of determination (r^2) from the leave-one-out cross-validation method, RMSE, and model bias.

A second evaluation of the PLSR model was performed with a holdout data set. In this case, 80% of the data were used as a training data set for the estimation of leaf traits, and 20% of the data were used as a testing data set.

For chlorophyll, N content, SLA, V_{max}, and $V_{p,max}$, training data sets were collected from both field-grown and greenhouse-grown maize plants. For these traits, two PLSR models were built, one with field-grown data only and a second with the entire training data set from the field and the greenhouse (Fig. 1). The better of the two PLSR models based on larger r^2 and smaller RMSE (typically the one with data from both the field and greenhouse) was then applied to the O_3 screening data set collected in the field in 2013, 2014, and 2015. The PLSR model coefficients for each trait are provided in Supplemental Table S1.

High-Throughput Screening for O_3 Response

As a test of the potential to use leaf reflectance spectra for high-throughput screening, diverse maize germplasm were measured in the FACE experiment described above in 2013, 2014, and 2015 (Supplemental Data Set S2). Leaf reflectance spectra were taken on the third youngest leaf with a collar from all experimental rows (1,024 in 2013, 768 in 2014, and 912 in 2015). In 2013 and 2014, two plants per genotype (row) were sampled within each ambient and elevated [O_3] ring, and in 2015, a single plant per row was sampled because each genotype was planted in five rows within each ring. Leaf reflectance was measured twice in 2013, from July 14 to 17 and July 29 to 30, and from July 14 to 18, 2014, and July 15 to 16, 2015.

Statistical Analysis of Measured and Predicted Trait Values

In addition to PLSR models, published indices for estimating chlorophyll content, N content, and SLA were tested using the training population (Table I). Correlations between published indices and measured values were tested. Pairwise correlations among the gold standard measured traits and the spectral-derived traits were tested using the training data set. The ability to distinguish statistical differences in measured and PLSR-modeled traits also was tested with a subset of the training data set. Measured and PLSR-modeled estimates of chlorophyll content, N content, V_{max}, and SLA from genotypes B73, Mo17, and B73 × Mo17 were used to test for the effects of genotype, O_3, and their interaction using a general linear model.

The field designs in 2013, 2014, and 2015 differed in the number of genotypes examined and the layout of the FACE and control rings among years. Models were fit for each year separately. For the 2013 data, the linear model $Y_{ijkl} = \mu + t_j + \rho_{ij} + g_k + tg_{ij} + \varepsilon_{ijkl}$ was fit, where j is the jth treatment (ambient, elevated [O_3]), i is the random effect of the ith ring pair ($i = 1,..4$), and k is the kth genotype. The variance of the ring pairs was assumed to be common for all ambient rings and all elevated [O_3] rings but not assumed to be the same between them, and an additional covariance parameter for the southwest corner of the rings was included. In 2014, $Y_{ijkl} = \mu + t_j + \rho_{ij} + g_k + tg_{ij} + \varepsilon_{ijkl}$ was fit, where j is the jth treatment, i is the random effect of the ith ring pair ($i = 1,..4$), and k is the kth genotype. The increased number of replicates in 2014 allowed us to fit the residuals for the difference in variance structure as $\varepsilon \sim N(0,\Sigma)$, where Σ is the variance covariance matrix with diagonal elements σ_j and all off-diagonal terms are zero except for a single covariance p to account for spatial variation among observations in the southwest quadrant of the elevated [O_3] rings. In 2015, the ring was divided into five sectors, i.e. northeast, northwest, southeast, southwest and central, and in each sector all of the genotypes were planted. The model $Y_{ijkl} = \mu + t_j + \rho_{ij} + \gamma_s(p_{ij}) + b_l + g_k + tg_{ij} + \varepsilon_{ijkl}$ was fit, where Y_{ijkl} is the trait value for the ith ring pair ($i = 1,..4$), the sth sector ($s = 1,\ldots5$) nested inside the ring pair for the jth treatment, the lth sector (1 for the sector in the southwest, 0 otherwise), and the kth genotype. Ring pair and sector are treated as random with all other effects fixed.

Supplemental Data

The following supplemental materials are available.

Supplemental Figure S1. Mean measured and PLSR-modeled leaf traits ± 1 SD for maize genotypes B73, B73 × Mo17, and Mo17.

Supplemental Figure S2. Bootstrap estimate of mean chlorophyll content and SD from one to 24 spectra taken on an individual leaf.

Supplemental Table S1. PLSR model coefficients for predicting foliar traits using leaf reflectance spectra from maize.

Supplemental Table S2. Performance comparison between predictive models built with either the entire training population (full model) or 80% of the training population (80% model).

Supplemental Table S3. ANOVA degrees of freedom, F value, and significance level for measured and PLSR-modeled leaf traits.

Supplemental Table S4. List of inbred and hybrid maize genotypes grown at ambient (approximately 40 nL L^{-1}) and elevated (approximately 100 nL L^{-1}) [O_3] in the 2013, 2014, and 2015 growing seasons.

Supplemental Table S5. Seasonal average daily [O_3] exposure at the SoyFACE facility in 2013, 2014, and 2015.

Supplemental Data Set S1. Raw spectral data for wavelengths used to build PLSR models, along with measured trait values and PLSR-predicted trait values.

Supplemental Data Set S2. Raw spectral data for the screening data set collected on diverse maize inbred and hybrid lines grown in the field in ambient and elevated [O_3] in 2013, 2014, and 2015.

ACKNOWLEDGMENTS

We thank Brad Dalsing, Chad Lantz, Kannan Puthuval, and Mac Singer for operating the SoyFACE facility and Matt Lyons, Dan Jaskowiak, John Regan, Anna Molineaux, Jessica Wedow, Taylor Pederson, Chris Moller, Charles Burroughs, and Ben Thompson for assistance with field sampling and laboratory measurements.

Received September 14, 2016; accepted November 10, 2016; published November 15, 2016.

LITERATURE CITED

Adjorlolo C, Cho MA, Mutanga O, Ismail R (2012) Optimizing spectral resolutions for the classification of C_3 and C_4 grass species, using wavelengths of known absorption features. J Appl Remote Sens **6:** 063560

Ainsworth EA, Beier C, Calfapietra C, Ceulemans R, Durand-Tardif M, Farquhar GD, Godbold DL, Hendrey GR, Hickler T, Kaduk J, et al (2008) Next generation of elevated [CO_2] experiments with crops: a critical investment for feeding the future world. Plant Cell Environ **31:** 1317–1324

Ainsworth EA, Serbin SP, Skoneczka JA, Townsend PA (2014) Using leaf optical properties to detect ozone effects on foliar biochemistry. Photosynth Res **119:** 65–76

Ainsworth EA, Yendrek CR, Sitch S, Collins WJ, Emberson LD (2012) The effects of tropospheric ozone on net primary productivity and implications for climate change. Annu Rev Plant Biol **63:** 637–661

Araus JL, Cairns JE (2014) Field high-throughput phenotyping: the new crop breeding frontier. Trends Plant Sci **19:** 52–61

Asner GP, Martin RE (2008) Spectral and chemical analysis of tropical forests: scaling from leaf to canopy levels. Remote Sens Environ **112:** 3958–3970

Asner GP, Martin RE (2015) Spectroscopic remote sensing of non-structural carbohydrates in forest canopies. Remote Sens **7:** 3526–3547

Asner GP, Martin RE, Knapp DE, Tupayachi R, Anderson C, Carranza L, Martinez P, Houcheime M, Sinca F, Weiss P (2011) Spectroscopy of canopy chemicals in humid tropical forests. Remote Sens Environ **115:** 3587–3598

Atzberger C, Guerif M, Baret F, Werner W (2010) Comparative analysis of three chemometric techniques for the spectroradiometric assessment of canopy chlorophyll content in winter wheat. Comput Electron Agric **73:** 165–173

Betzelberger AM, Yendrek CR, Sun J, Leisner CP, Nelson RL, Ort DR, Ainsworth EA (2012) Ozone exposure response for U.S. soybean cultivars: linear reductions in photosynthetic potential, biomass, and yield. Plant Physiol **160:** 1827–1839

Brosché M, Merilo E, Mayer F, Pechter P, Puzõrjova I, Brader G, Kangasjärvi J, Kollist H (2010) Natural variation in ozone sensitivity among *Arabidopsis thaliana* accessions and its relation to stomatal conductance. Plant Cell Environ **33:** 914–925

Chen S, Hong X, Harris CJ, Sharkey PM (2004) Sparse modeling using orthogonal forward regression with PRESS statistic and regularization. IEEE Trans Syst Man Cybern B Cybern **34:** 898–911

Cheng T, Rivard B, Sanchez-Azofeifa AG, Feret JB, Jacquemoud S, Ustin SL (2014) Deriving leaf mass per area (LMA) from foliar reflectance across a variety of plant species using continuous wavelet analysis. ISPRS J Photogramm Remote Sens **87:** 28–38

Christensen JH, Hewitson B, Busuioc A, Chen A, Gao X, Held I, Jones R, Kolli RK, Kwon WT Laprise R, et al (2007) Regional climate projections. *In* S Solomon, D Qin, M Manning, Z Chen, M Marquis, KB Averyt, M Tignor, HL Miller, eds, Climate Change 2007: The Physical Science Basis. Contribution of Working Group I to the Fourth Assessment Report of the Intergovernmental Panel on Climate Change. Cambridge University Press, Cambridge, UK, pp 847–940

Curran PJ (1989) Remote sensing of foliar chemistry. Remote Sens Environ **30:** 271–278

Datt B (1998) Remote sensing of chlorophyll *a*, chlorophyll *b*, chlorophyll *a* +*b* and total carotenoid content in eucalyptus leaves. Remote Sens Environ **66:** 111–121

Dhondt S, Wuyts N, Inzé D (2013) Cell to whole-plant phenotyping: the best is yet to come. Trends Plant Sci **18:** 428–439

Dizengremel P, Le Thiec D, Bagard M, Jolivet Y (2008) Ozone risk assessment for plants: central role of metabolism-dependent changes in reducing power. Environ Pollut **156:** 11–15

Dodd AN, Salathia N, Hall A, Kévei E, Tóth R, Nagy F, Hibberd JM, Millar AJ, Webb AAR (2005) Plant circadian clocks increase photosynthesis, growth, survival, and competitive advantage. Science **309:** 630–633

Doughty CE, Asner GP, Martin RE (2011) Predicting tropical plant physiology from leaf and canopy spectroscopy. Oecologia **165:** 289–299

Dreccer MF, Barnes LR, Meder R (2014) Quantitative dynamics of stem water soluble carbohydrates in wheat can be monitored in the field using hyperspectral reflectance. Field Crops Res **159:** 70–80

Farquhar GD, von Caemmerer S, Berry JA (1980) A biochemical model of photosynthetic CO_2 assimilation in leaves of C_3 species. Planta **149:** 78–90

Fiscus EL, Booker FL, Burkey KO (2005) Crop responses to ozone: uptake, modes of action, carbon assimilation and partitioning. Plant Cell Environ **28:** 997–1011

Frei M, Tanaka JP, Wissuwa M (2008) Genotypic variation in tolerance to elevated ozone in rice: dissection of distinct genetic factors linked to tolerance mechanisms. J Exp Bot **59:** 3741–3752

Furbank RT, Tester M (2011) Phenomics: technologies to relieve the phenotyping bottleneck. Trends Plant Sci **16:** 635–644

Gamon JA, Serrano L, Surfus JS (1997) The photochemical reflectance index: an optical indicator of photosynthetic radiation use efficiency across species, functional types, and nutrient levels. Oecologia **112:** 492–501

Gillespie KM, Chae JM, Ainsworth EA (2007) Rapid measurement of total antioxidant capacity in plants. Nat Protoc **2:** 867–870

Gillespie KM, Xu F, Richter KT, McGrath JM, Markelz RJC, Ort DR, Leakey ADB, Ainsworth EA (2012) Greater antioxidant and respiratory metabolism in field-grown soybean exposed to elevated O_3 under both ambient and elevated CO_2. Plant Cell Environ **35:** 169–184

Gitelson AA, Buschmann C, Lichtenthaler HK (1999) The chlorophyll fluorescence ratio F735/F700 as an accurate measure of the chlorophyll content in plants. Remote Sens Environ **69:** 296–302

Gitelson AA, Merzlyak MN (1997) Remote estimation of chlorophyll content in higher plant leaves. Int J Remote Sens **18:** 2691–2697

Großkinsky DK, Svensgaard J, Christensen S, Roitsch T (2015) Plant phenomics and the need for physiological phenotyping across scales to narrow the genotype-to-phenotype knowledge gap. J Exp Bot **66:** 5429–5440

Hansen PM, Schjoerring JK (2003) Reflectance measurement of canopy biomass and nitrogen status in wheat crops using normalized difference vegetation indices and partial least squares regression. Remote Sens Environ **86:** 542–553

Herrmann I, Karnieli A, Bonfil DJ, Cohen Y, Alchanatis V (2010) SWIR-based spectral indices for assessing nitrogen content in potato fields. Int J Remote Sens **31:** 5127–5143

Hewitt EJ, Smith TA (1975) Plant Mineral Nutrition. English Universities Press, London

Irisarri JGN, Oesterheld M, Verón SR, Paruelo JM (2009) Grass species differentiation through canopy hyperspectral reflectance. Int J Remote Sens **22:** 5959–5975

Jacquemoud S, Baret F (1990) PROSPECT: a model of leaf optimal properties spectra. Remote Sens Environ **34:** 75–91

Jones MGK, Outlaw WH, Lowry OH (1977) Enzymic assay of 10 to 10 moles of sucrose in plant tissues. Plant Physiol **60:** 379–383

Kim KM, Kwon YS, Lee JJ, Eun MY, Sohn JK (2004) QTL mapping and molecular marker analysis for the resistance of rice to ozone. Mol Cells **17:** 151–155

Kraft M, Weigel HJ, Mejer GJ, Brandes F (1996) Reflectance measurements of leaves for detecting visible and non-visible damage to crops. J Plant Physiol **148:** 148–154

Leitao L, Bethenod O, Biolley JP (2007) The impact of ozone on juvenile maize (*Zea mays* L.) plant photosynthesis: effects on vegetative biomass, pigmentation, and carboxylases (PEPc and Rubisco). Plant Biol (Stuttg) **9:** 478–488

le Maire G, Francois C, Dufrene E (2004) Towards universal broad leaf chlorophyll indices using PROSPECT simulated database and hyperspectral reflectance measurements. Remote Sens Environ **89:** 1–28

le Maire G, Francois C, Soudani K, Berveiller D, Pontailler JY, Breda N, Genet H, Davi H, Dufrene E (2008) Calibration and validation of hyperspectral indices for the estimation of broadleaved forest leaf chlorophyll content, leaf mass per area, leaf area index and leaf canopy biomass. Remote Sens Environ **112:** 3846–3864

Lichtenthaler HK, Wellburn AR (1983) Determination of total carotenoids and chlorophylls a and b of leaf extracts in different solvents. Biochem Soc Trans **11:** 591–592

Liu L, Cheng Z (2011) Mapping C_3 and C_4 plant functional types using separated solar-induced chlorophyll fluorescence from hyperspectral data. Int J Remote Sens **32:** 9171–9183

Maccioni A, Agati G, Mazzinghi P (2001) New vegetation indices for remote measurement of chlorophylls based on leaf directional reflectance spectra. J Photochem Photobiol B **61:** 52–61

Markelz RJC, Strellner RS, Leakey ADB (2011) Impairment of C_4 photosynthesis by drought is exacerbated by limiting nitrogen and ameliorated by elevated [CO_2] in maize. J Exp Bot **62:** 3235–3246

Martin ME, Aber JD (1997) High spectral resolution remote sensing of forest canopy lignin, nitrogen and ecosystem processes. Ecol Appl **7:** 431–443

McGrath JM, Betzelberger AM, Wang S, Shook E, Zhu XG, Long SP, Ainsworth EA (2015) An analysis of ozone damage to historical maize and soybean yields in the United States. Proc Natl Acad Sci USA **112:** 14390–14395

McMullen MD, Kresovich S, Villeda HS, Bradbury P, Li H, Sun Q, Flint-Garcia S, Thornsberry J, Acharya C, Bottoms C, et al (2009) Genetic properties of the maize nested association mapping population. Science **325:** 737–740

McMurtey JE III, Chapelle EW, Kim MS, Meisinger JJ, Corp LA (1994) Distinguishing nitrogen fertilization levels in field corn (*Zea mays* L.) with actively induced fluorescence and passive reflectance measurements. Remote Sens Environ **47:** 36–44

Meroni M, Panigada C, Rossini M, Picchi V, Cogliati S, Colombo R (2009) Using optical remote sensing techniques to track the development of ozone-induced stress. Environ Pollut **157:** 1413–1420

Mevik BH, Wehrens R (2007) The pls package: principal component and partial least squares regression in R. J Stat Softw **18:** 1–24

Miller JD, Arteca RN, Pell EJ (1999) Senescence-associated gene expression during ozone-induced leaf senescence in Arabidopsis. Plant Physiol **120:** 1015–1024

Morgan PB, Bernacchi CJ, Ort DR, Long SP (2004) An in vivo analysis of the effect of season-long open-air elevation of ozone to anticipated 2050 levels on photosynthesis in soybean. Plant Physiol **135:** 2348–2357

Penuelas J, Baret F, Filella I (1995) Semi-empirical indices to assess carotenoids/chlorophyll *a* ratio from leaf spectral reflectance. Photosynthetica **31:** 221–230

Penuelas J, Filella I (1998) Visible and near-infrared reflectance techniques for diagnosing plant physiological status. Trends Plant Sci **3:** 151–156

Poorter H, Niklas KJ, Reich PB, Oleksyn J, Poot P, Mommer L (2012) Biomass allocation to leaves, stems and roots: meta-analyses of interspecific variation and environmental control. New Phytol **193:** 30–50

Reich PB, Amundson RG (1985) Ambient levels of ozone reduce net photosynthesis in tree and crop species. Science **230:** 566–570

Reich PB, Walters MB, Ellsworth DS (1997) From tropics to tundra: global convergence in plant functioning. Proc Natl Acad Sci USA **94:** 13730–13734

Richardson AD, Reeves JB (2005) Quantitative reflectance spectroscopy as an alternative to traditional wet lab analysis of foliar chemistry: near-infrared and mid-infrared calibrations compared. Can J Res **35:** 1122–1130

Rudorff BFT, Mulchi CL, Daughtry CST, Lee EH (1996) Growth, radiation use efficiency, and canopy reflectance of wheat and corn grown under elevated ozone and carbon dioxide atmospheres. Remote Sens Environ **55:** 163–173

Runeckles VC, Resh HM (1975) The assessment of chronic ozone injury to leaves by reflectance spectrophotometry. Atmos Environ **9:** 447–452

Serbin SP, Dillaway DN, Kruger EL, Townsend PA (2012) Leaf optical properties reflect variation in photosynthetic metabolism and its sensitivity to temperature. J Exp Bot **63:** 489–502

Serbin SP, Singh A, Desai AR, Dubois SG, Jablonski AD, Kingdon CC, Kruger EL, Townsend PA (2015) Remotely estimating photosynthetic capacity, and its response to temperature, in vegetation canopies using imaging spectroscopy. Remote Sens Environ **167:** 78–87

Serbin SP, Singh A, McNeil BE, Kingdon CC, Townsend PA (2014) Spectroscopic determination of leaf morphological and biochemical traits for northern temperate and boreal tree species. Ecol Appl **24:** 1651–1669

Serrano L, Penuelas J, Ustin SL (2002) Remote sensing of nitrogen and lignin in Mediterranean vegetation from AVIRIS data: decomposing biochemical from structural signals. Remote Sens Environ **81:** 355–364

Siegmann B, Jarmer T (2015) Comparison of different regression models and validation techniques for the assessment of wheat leaf area index from hyperspectral data. Int J Remote Sens **36:** 4519–4534

Sims DA, Gamon JA (2002) Relationships between leaf pigment content and spectral reflectance across a wide range of species, leaf structures and developmental stages. Remote Sens Environ **81:** 337–354

Street NR, James TM, James T, Mikael B, Jaakko K, Mark B, Taylor G (2011) The physiological, transcriptional and genetic responses of an ozone-sensitive and an ozone tolerant poplar and selected extremes of their F2 progeny. Environ Pollut **159:** 45–54

Tilman D, Balzer C, Hill J, Befort BL (2011) Global food demand and the sustainable intensification of agriculture. Proc Natl Acad Sci USA **108:** 20260–20264

Ueda Y, Siddique S, Frei M (2015) A novel gene, OZONE-RESPONSIVE APOPLASTIC PROTEIN1, enhances cell death in ozone stress in rice. Plant Physiol **169:** 873–889

Vogelmann JE, Rock BN, Moss DM (1993) Red edge spectral measurements from sugar maple leaves. Int J Remote Sens **14:** 1563–1575

von Caemmerer S (2000) Biochemical Models of Leaf Photosynthesis. CSIRO Publishing, Collingwood, Australia

Weber VS, Araus JL, Cairns JE, Sanchez C, Melchinger AE, Orsini E (2012) Prediction of grain yield using reflectance spectra of canopy and leaves in maize plants grown under different water regimes. Field Crops Res **128:** 82–90

Wold S (1994) PLS for multivariate linear modeling. *In* H van de Waterbeernd, ed, Chemometric Methods in Molecular Design, Methods and Principles in Medicinal Chemistry. Verlag-Chemie, Weinheim, Germany, pp 195–218

Wold S, Sjostrom M, Eriksson L (2001) PLS-regression: a basic tool of chemometrics. Chemometr Intell Lab **58:** 109–130

Wright IJ, Reich PB, Westoby M, Ackerly DD, Baruch Z, Bongers F, Cavender-Bares J, Chapin T, Cornelissen JHC, Diemer M, et al (2004) The worldwide leaf economics spectrum. Nature **428:** 821–827